JOURNAL OF CATALYSIS **158,** 83–91 (1996)
ARTICLE NO. 0008

Oxidation of Methane to Synthesis Gas in a Fluidized Bed Reactor Using MgO-Based Catalysts

A. Santos,* M. Menéndez,* A. Monzón,* J. Santamaria,*,[1] E. E. Miró,† and E. A. Lombardo†

*Department of Chemical and Environmental Engineering, University of Zaragoza, 50009 Zaragoza, Spain; and †Instituto de Investigaciones en Catálisis y Petroquímica, INCAPE (FIQ-UNL-CONICET), Santiago del Estero 2829-3000, Santa Fe, Argentina

Received December 28, 1994; revised May 12, 1995; accepted July 26, 1995

Ni(15%)/MgO and Co(12%)/MgO have been used as catalysts to carry out the oxidation of methane to synthesis gas in a fluidized-bed reactor. The fresh and used catalysts have been characterized through a battery of instrumental techniques aiming at finding the relationship among the operating conditions, activity, and stability of the reacting system. The fresh catalysts are made up of a mixture of crystalline MgO and $MgMO_2$ (M = Ni or Co) while the used ones also contain NiO and CoO. This explains the on-stream activation of the solid in terms of an *in situ* reduction of the oxides to generate the metallic centers needed to catalyze the reforming reaction. Under some of the experimental conditions employed, the SEM micrographs of the used solids show coke formation in whiskers. These will be burnt in the oxidizing zone of the fluidized bed, thus releasing Ni particles, which may be deposited on the freeboard walls. These metallic particles can catalyze back reactions, decreasing the overall yield to the desired reaction products, CO and H_2.

INTRODUCTION

An active search has been under way in the last several years to find selective processes for the direct conversion of methane to either C^{2+} hydrocarbons or oxygenated compounds (methanol–formaldehyde). So far, however, the yields attainable through both of these processes are not enough to justify commercial application. This has spurred research trying to find more efficient reactors (e.g., (1)) and better catalysts (e.g., (2)) for the above processes.

A different alternative utilization of natural gas as a feedstock involves the use of steam reforming or oxidation processes to obtain synthesis gas, which is then transformed using the appropriate route (e.g., obtaining of α-olefins via Fisher–Tropsch synthesis). Recently, a number of authors (e.g. (3–6)), have shown that the production of synthesis gas through the catalytic oxidation of methane is a promising alternative to steam reforming. In this way, it is possible to reach near equilibrium conversions while at the same time avoiding the need for an external heat input, since on the whole the process of methane oxidation to syngas is mildly exothermic. However, while high conversions can be obtained at atmospheric pressure, the economics of the process seem to be favorable at high pressures (7), which implies much lower equilibrium conversions. This has led to the use of membrane reactors (8) as a way to circumvent equilibrium limitations.

There is experimental evidence (5, 9) which indicates that, under certain conditions (e.g., temperatures higher than 1000°C, very short contact times, and Pt or Rh catalysts), the catalytic partial oxidation of methane to synthesis gas may take place directly. However, under the conditions employed in most of the laboratory studies reported, the oxidation of methane to synthesis gas seems to occur through the combustion to CO_2 plus H_2O of a portion of the methane feed, followed by steam and CO_2 reforming of the remaining methane (e.g., (10–12)). Due to the high reaction rates involved and the exothermicity of the methane combustion in the oxygen-rich zone, it is likely that significant temperature gradients are originated in the reactor. These gradients may originate hot spots in the catalyst bed which will interfere with the interpretation of laboratory data (13) and will surely cause operation difficulties in industrial reactors.

Also, the deactivation of the catalyst by carbon deposition is often a problem in this system. Claridge *et al.* (14) have reported that the rate of carbon deposition in group VIII metals follows the order Ni > Pd > Rh > Ir. They also found that methane decomposition and not the Boudouard reaction is the main route leading to carbon deposition on nickel-containing catalysts.

The fluid-bed reactor is an attractive alternative for this process because it provides the high heat transfer rates needed to maintain isothermal operation (15), and also because the permanent circulation of the catalyst particles favors carbon burning in the oxygen-rich zone of the bed. In fact, Santos *et al.* (16) using Ni/Al_2O_3 as a syngas catalyst

[1] To whom correspondence should be addressed. E-Mail: IQCATAL@CC.UNIZAR.ES.

0021-9517/96 $12.00

in a fluidized bed found only 0.6 wt% of carbonaceous deposit on the solid after a 10-h operation period at 800°C. Under similar operating conditions in a tubular flow reactor, it has been reported that the catalyst contained up to 40 wt% of carbon (14).

So far, relatively few papers have been published using fluid-bed reactors. Olsbye *et al.* (15), Santos *et al.* (16) and Bharadwaj and Schmidt (17) have reported near equilibrium conversions and selectivities with almost homogeneous bed temperature. However, the entrainment of catalyst fines in the lower temperature freeboard zone favored back reactions and lowered the overall process yield. This was particularly the case when Ni/Al_2O_3 was the catalyst employed (15, 16).

The catalysts usually employed for the oxidation of methane to synthesis gas are active for both the total oxidation of methane and the reforming reactions. The active sites for the reforming reaction may be generated *in situ*, e.g., metallic centers on supported oxides. Within this group, solids made up of nickel oxide or cobalt oxide deposited or coprecipitated with MgO are active for these reactions (18, 19).

In this work Ni/MgO and Co/MgO have been used as catalysts in a fluid-bed reactor similar to the one described by Santos *et al.* (16). The fresh and used catalysts have been characterized through X-ray diffraction (XRD), X-ray photoelectron spectroscopy (XPS), temperature programmed reduction (TPR) and scanning electron microscopy (SEM), with the aim of studying the relationship among the operating conditions, activity, and stability of the reacting system.

EXPERIMENTAL

Catalysts Preparation and Characterization

Ni/MgO and Co/MgO solids were prepared from 50 g of MgO which were mixed with 250 cm^3 of aqueous solutions of cobalt or nickel nitrates. Samples with 15 wt% of nickel and 12 wt% of cobalt were obtained. The salts employed in the impregnation and MgO were Merck pro-analysis. The slurry obtained was vigorously stirred for 2 h at room temperature and then evaporated, while still stirring at 70°C until achieving a thick paste. The said paste was dried in an oven, at 120°C, for 24 h. The solids were then calcined in air at 800°C in a rotatory oven for 12 h. Catalysts thus prepared were pelletized, ground, and screened between 80 and 150 mesh.

The BET area of each catalyst was measured after calcination, but prior to the reaction, using a Micromeritics Flow Sorb 2000 sorptometer. The pore volume of the calcined samples was measured with an Autopore II 9220 V2.03 mercury porosimeter (Table 1). The characterization of the crystalline phases was performed through XRD with a Shimadzu XD-D1 instrument, using Ni filtered Cu$K\alpha$ radiation.

TABLE 1

Physical Properties of Catalysts

Catalysts	Ni	Co wt.%	BET surface area (m^2/g)	Average pore size (nm)	Skeletal density	Particle porosity
Ni/MgO	15	—	31.0	35	3.3	46.3
Co/MgO	—	12	14.4	50	3.7	50.9

The XPS spectra were obtained at room temperature with a computer-controled Shimadzu ESCA 750 instrument, using Mg$K\alpha$ radiation. The Ni/Mg and Co/Mg atomic ratios were calculated using the area under the Mg2p, Ni2$p_{3/2}$ and Co2$p_{3/2}$ peaks, the Scofield photoionization cross-sections, the mean free paths of the electrons and the instrument function which was given by the ESCA manufacturer. The binding energies (BEs) were always referred to Mg2p of the MgO at 50.8 eV (21).

Temperature-programmed reduction experiments were carried out on 0.2 g samples using a 5.7% hydrogen in nitrogen mixture. The gas flow was 106 cm^3/min and the temperature was raised at 10 K/min from room temperature to 1173 K.

The catalyst surface was examined using a JEOL JSM 6400 scanning electron microscope, both on fresh and on used catalyst samples. This allowed an assessment of the morphology of the catalyst surface and of the extent of coke formation in whiskers.

Reaction Experiments

A 30-mm-i.d., 235-mm-long fused quartz reactor has been used in all the experiments. The reactor is equipped with a sintered quartz distributor plate and a quartz thermowell in the bubbling zone, which was used for the control thermocouple. In addition, an opening at the top of the reactor could be used to insert a movable quartz probe to take gas samples at different bed heights. Alternatively, the quartz probe could be replaced by a quartz thermowell in order to monitor temperature profiles. The position of the reactor relative to the external electrical furnace could be modified in order to create different temperature profiles in the freeboard region of the reactor. Two different relative positions were used, namely position 1 in which approximately 85% of the reactor length was heated, and position 2, in which the reactor was partly slid out of the furnace and only 66% of its length was heated. More details about this reacting system have been given elsewhere (16).

The typical catalyst loading was 25 g, with an average particle size of approximately 140 and 130 μm for the Ni/MgO and Co/MgO catalysts, respectively. The minimum

TABLE 2

XRD Main Phases and Hydrogen Consumption in TPR Experiments in Fresh[a] and Used[b] Catalysts

Catalysts	XRD Ni and Co main phases	Hydrogen consumption (mmol/g)
Fresh catalysts		
Ni/MgO	$MgNiO_2$	(<0.05)
Co/MgO	$MgCoO_2$	(<0.05)
Used catalysts		
Ni/MgO	$MgNiO_2$, $MgNi_4O_6$, NiO	1.1
Co/MgO	$MgCoO_2$, CoO	0.36

[a] Solids calcined at 800°C.
[b] After reaction and coke burning at 500°C.

fluidization velocity was determined using nitrogen at the reaction temperature, and then corrected to account for the different density and viscosity of the reaction mixture. Using this method, a value of 0.42 and 0.27 cm/s at the reaction conditions was found respectively for the Ni/MgO and Co/MgO catalysts. Reduced velocities of 3 and 4.8 were used in all the experiments reported in this work for the Ni/MgO and Co/MgO catalysts respectively. Under these conditions, the height of the bubbling zone was typically about 8 cm, and the length of the freeboard was 15.5 cm. Attrition and agglomeration problems were avoided by optimization of the catalyst particle size. The loss of catalyst fines by elutration was negligible after more than 20 h on stream.

$CH_4/O_2/N_2$ mixtures were fed to the reactor by using mass flow controllers, at reaction temperatures between 200 and 900°C. Different W/F and reactant feed ratios were investigated, although the most frequently used conditions were $F = 500$ cm^3 (STP)/min and $CH_4/O_2/N_2 = 2/1/1$.

The product gases were analyzed by on-line gas chromatography. The carbon balance closures were always better than 95%. The amount of carbon deposited on the catalyst after an experiment was determined by burning off the deposits with air and measuring the total amounts of CO and CO_2 formed using gas chromatography.

RESULTS

Catalyst Characterization

The X-ray diffraction patterns show that the fresh catalysts are made up of MgO and mixed oxides, either $MgNiO_2$ or $MgCoO_2$ (Table 2). Neither nickel nor cobalt crystalline oxides were detected in these patterns. Besides, the TPR thermograms do not show any well-defined reduction peak up to 900°C. This is expected for $MgNiO_2$ and $MgCoO_2$ are much more difficult to reduce than the single cobalt and nickel oxides. On line with these findings, both the Ni2$p_{3/2}$ and Co2$p_{3/2}$ BEs are 2 eV higher than those corresponding to nickel oxide and cobalt oxide (Table 3). The BEs for the mixed oxides could not be found in the literature. The closest compounds for which XPS data have been reported by several authors are the corresponding aluminates. Our BEs for Ni2$p_{3/2}$ and Co2$p_{3/2}$ are higher than those reported for the aluminates, particularly so in the latter case. No explanation for these high BE values can be given at this time. Whatever the reason for the high BE values found, the comparison between the XPS spectra of fresh and used Ni/MgO and Co/MgO catalysts (Figs. 1a and 1b, respectively), are useful to assess the changes occurred in the course of reaction.

The used catalysts have been on stream for more than 20 h at 700–900°C. The surface coke was then burnt in oxygen at 500°C. Analysis of the fresh and used samples showed that these solids did not lose a significant amount of metal during use. However, XPS results showed a 30–40% decrease on the surface values of both Ni/Mg and Co/Mg ratios for the used samples (Table 3). Also, the BEs of Ni2$p_{3/2}$ and Co2$p_{3/2}$ were coincident with those of the fresh catalysts but the peaks became significantly wider (Fig. 1). The peak widening which tails off towards the lower BE region, particularly in Co/MgO, is symptomatic of the presence of nickel oxide and cobalt oxide. In the latter case, it was possible, through curve fitting, to calculate that the cobalt oxide peak contribution was roughly 11%. The TPR thermograms of the used catalysts showed the presence of reduction peaks at 350–400°C which confirms the presence of the single oxides. Based upon area calculations, the molar percentage of the single oxides is ca. 42% and ca. 14% for Ni and Co respectively. The presence of the oxides is further documented in the X-ray patterns of the used catalysts (Table 2).

With the aim of studying the structure of the coke formed on these catalysts, the reaction was carried out for

TABLE 3

XPS Analysis of Fresh and Used Catalysts

Catalysts	BE (eV)[a]		Atomic ratios[b]	
	Ni2$p_{3/2}$	Co2$p_{3/2}$	Ni/Mg	Co/Mg
Fresh catalysts				
Ni/MgO	857.8(3.0)[c]	—	0.16	—
Co/MgO	—	782.8(4.0)	—	0.24
Used catalysts				
Ni/MgO	857.6(4.1)	—	0.11	—
Co/MgO	—	782.6(5.2)	—	0.14

[a] Mg2p = 50.8 eV was used as reference [see reference (21)].
[b] See Experimental.
[c] Peak width at 50% of the maximum height.

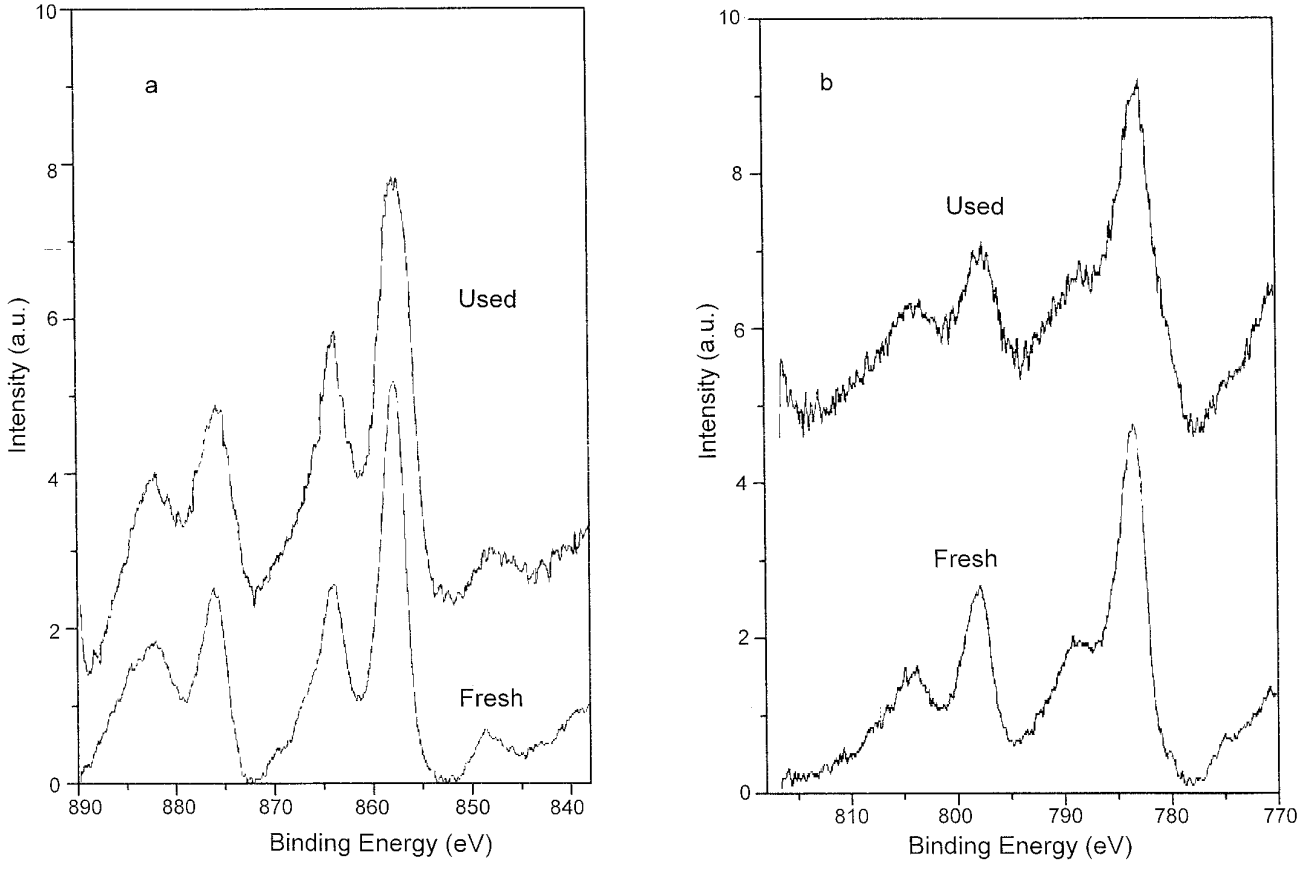

FIG. 1. XPS spectra of fresh and used catalysts. (a) Ni/MgO. (b) Co/MgO.

3 hours at 800°C with a CH_4/O_2 ratio of 3, which was expected to produce significant coke formation. Figure 2 shows the SEM micrographs obtained for both Ni/MgO and Co/MgO catalysts. It can be seen that a profuse formation of coke in whiskers takes place.

Kinetic Results

Experiments were conducted in the fluidized bed reactor under different temperatures and reactant feed ratios. Figure 3 shows the evolution of the reaction rate with temperature for the Co/MgO catalyst, starting at the lowest temperature and with the unreduced solid. A very similar behavior (not shown), was obtained for the Ni/MgO catalyst, and analogous results have been reported in the literature (3–5) using fixed-bed reactors. Between 400° and 800°C, the products detected were almost exclusively CO_2 and H_2O but when the temperature was increased to 800–900°C the reaction rate increased strongly, and the product distribution shifted. At 900°C, the measured CH_4 conversion was approximately 96% for Ni/MgO and 98% for Co/MgO, and the selectivities to CO and H_2 reached values close to thermodynamic equilibrium in both cases. When decreasing the temperature, the conversions, selectivities and reaction rates returned to the previous values by a different path, thus giving rise to the hysteresis curves of Fig. 3.

Figure 4a shows the reactor temperature profiles obtained using a Ni/MgO catalyst, for the two positions of the furnace referred in the Experimental section, and Fig. 4b, the corresponding methane conversion profile along the reactor. It can be seen that the methane conversion profile is at approximately the equilibrium value inside the bubbling fluidized bed and presents a very small decrease in the freeboard. Unlike previous results obtained with Ni/Al_2O_3 catalysts, in which both the conversion and selectivities were significantly affected by the furnace position (16), Fig. 4b shows that the methane conversion profile obtained with Ni/MgO catalysts was not significantly modified by changing the oven position between positions 1 and 2, in spite of important variations in the temperature profile of the freeboard (Fig. 4a). The Co/MgO catalyst yielded essentially the same results (not shown) as the Ni/MgO catalyst. Also, there was no significant effect on the CO and H_2 selectivities in both cases. The absence of the effect of lower freeboard temperatures that was present with Ni/Al_2O_3 catalysts (16), may be related to the fact that the catalysts used in this work had higher apparent densities

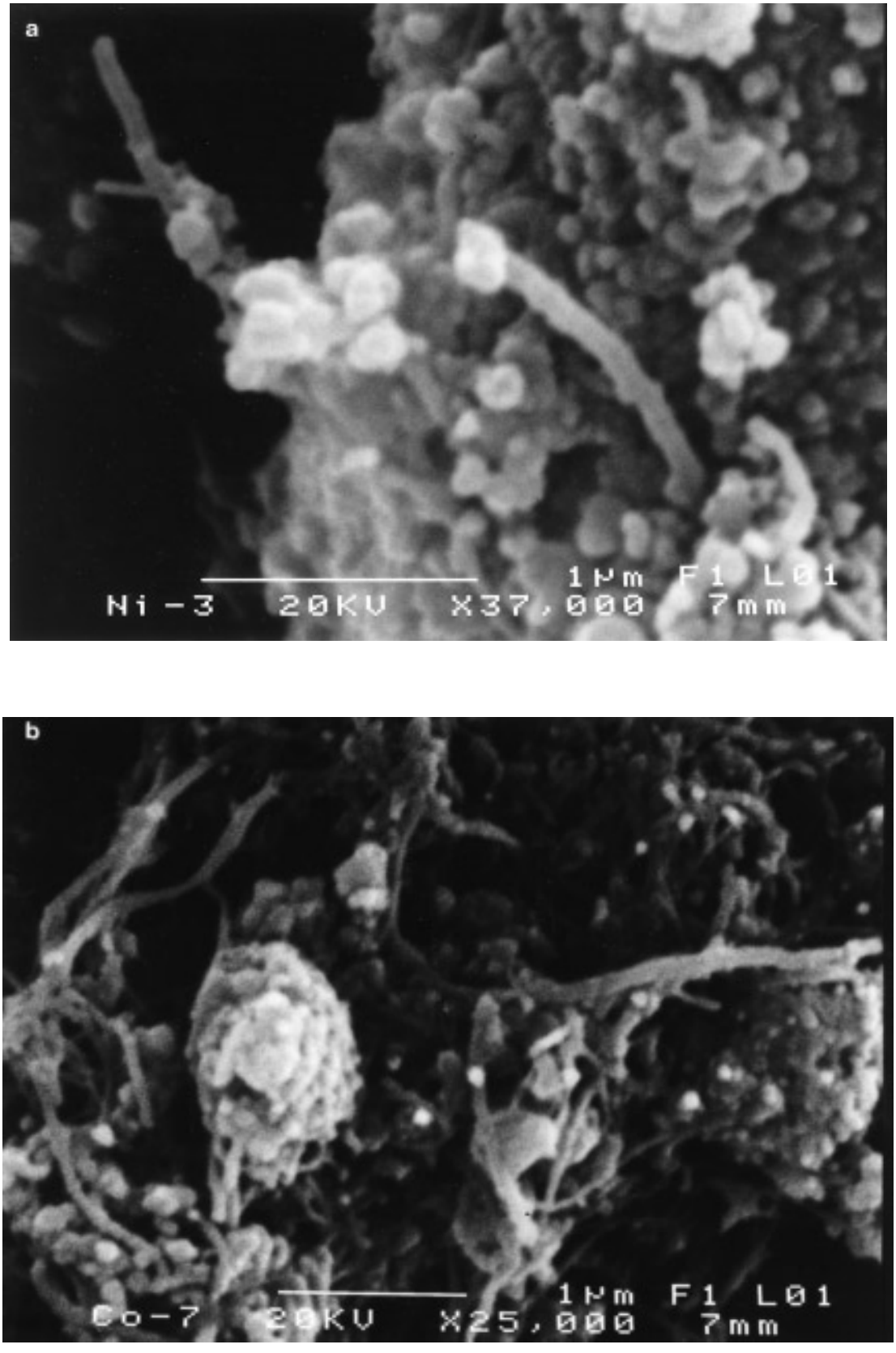

FIG. 2. SEM micrographs of catalyst samples after 3 h of time-on-stream. Reaction conditions: Temperature, 800°C; total flow rate, 500 cm^3/min; $CH_4:O_2 = 3:1$. (a) Ni/MgO. (b) Co/MgO.

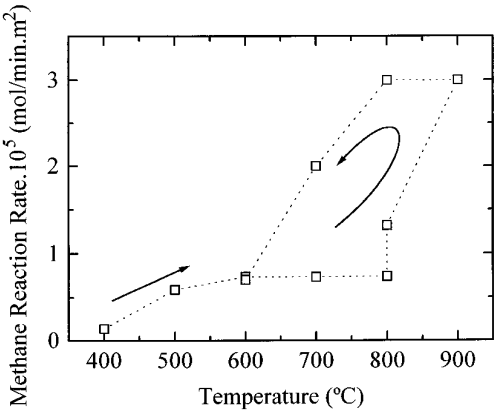

FIG. 3. Effect of temperature on methane conversion with $CH_4:O_2 = 2:1$. Other reaction conditions as in Table 1 with the Co/MgO catalyst. The arrows indicate the sequence followed to carry out the experiments.

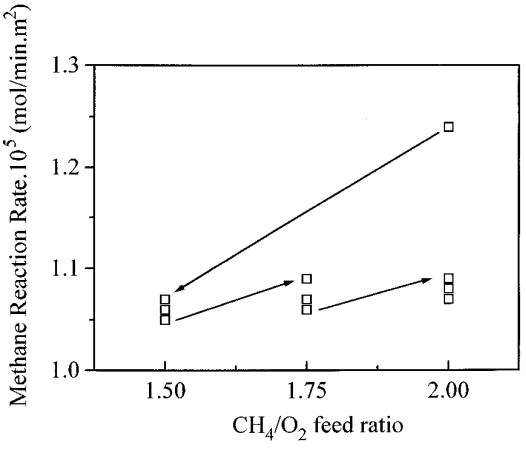

FIG. 5. Effect of the methane-to-oxygen ratio upon the reaction rate. Reactor conditions as in Fig. 3 with the Ni/MgO catalyst.

than the Ni/Al_2O_3 catalyst (especially in the case of the Co/MgO catalyst, with a 56% higher density), and therefore they are less likely to be entrained into the colder zone of the freeboard.

After an initial transient period, the reactor performance was constant for several hours of operation, as long as the inlet reactor conditions remained at a CH_4/O_2 ratio of 2. However, an important change in behavior was observed when the CH_4/O_2 ratio was changed back and forth between 2 and 1.5. Figure 5 shows that, after decreasing the CH_4/O_2 ratio to 1.5, the observed reaction rate decreased in successive samples taken every 20–30 min. When the CH_4/O_2 ratio was stepped first to 1.75 and then to 2, the observed reaction rate temporarily increased (since more methane was fed to the reactor). However, maintaining the feed at CH_4/O_2 ratios of 1.75 or 2, again led to a decrease in the observed reaction rate. The same trend was observed for the methane conversions and for the selectivities to CO and H_2.

It must be noticed that the data reported in Fig. 5 were obtained at the reactor exit, that is, after the gases exiting the bed had passed through the freeboard section. When gas samples were taken with the probe inserted in the bubbling zone at a height of 4 cm (not shown), the conversion and selectivity recovered the same value obtained at the beginning of the experiment. This rules out catalyst deactivation by coke as the cause of the observed decrease in conversion at the reactor exit. Also, since the conversion inside the fluidized bed is still at its previous value, while a lower conversion is obtained at the reactor exit, the reactions in the freeboard must be responsible for the observed decrease.

Santos *et al.* (16) reported that the entrainment of their catalyst, (Ni/Al_2O_3), was responsible for the reactions in the freeboard. This does not seem to take place in this

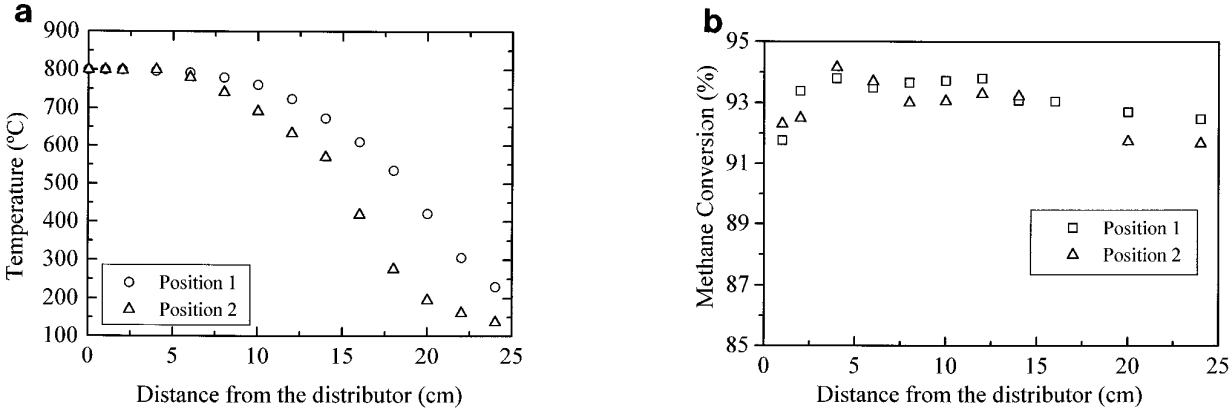

FIG. 4. (a) Temperature profiles in the bed at two different reactor-furnace positions. (b) Methane conversion profile along the reactor. Reactor conditions as in Fig. 3 with the Ni/MgO catalyst.

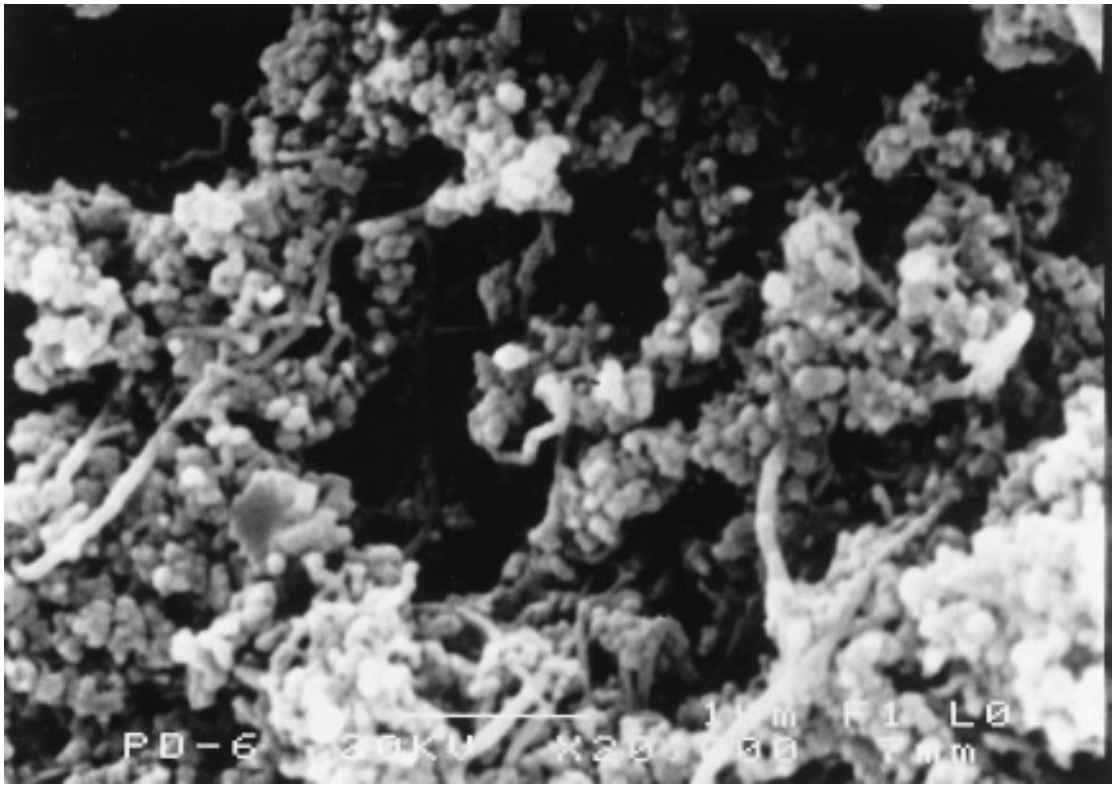

FIG. 6. SEM micrograph of deposits on the reactor walls (freeboard zone). The sample was taken after the run shown in Fig. 5.

work, as can be deduced from the results in Fig. 4. However, after the experiment corresponding to Fig. 5 was over, a black deposit appeared on the walls of the freeboard. The chemical analysis of this deposit indicated that it contained approximately 20% more nickel than the original catalyst. Also, SEM micrographs showed the presence of both whiskers and metal particles deposited on the freeboard walls (Fig. 6). The presence of active catalyst in the lower temperature regions of the reactor would certainly be an important factor to explain the back reactions leading to a decreased methane conversion at the reactor exit.

To further investigate the origin of the deposits on the reactor wall, the carbon deposits were burnt *in situ* by heating the reactor to 500°C in flowing air. From the amount of CO + CO_2 formed it was calculated that the catalyst had 0.52 wt% of coke. After coke burning was complete, the catalyst was discharged, the reactor was thoroughly cleaned to remove the black deposits on the wall, the catalyst was loaded back onto the reactor and the reaction was restarted. The results (not shown) reproduced the original performance of the catalyst. Furthermore, approximately the same results were obtained with catalyst loadings of 15 and 25 g, thus showing that the equilibrium is rapidly reached inside the bubbling zone of the fluidized bed.

A new set of reaction experiments using a variable CH_4/O_2 feed ratio was carried out with an aged nickel catalyst, which had been used in our laboratory for about 65 hours, and subjected to 3 intermediate regenerations with air. Figure 7 shows that for a CH_4/O_2 ratio of 2 the catalyst displayed a stable performance. When the CH_4/O_2 feed ratio was increased to 2.5, the reaction rate showed slowly decreasing values, which indicate an ongoing process of coke deposition on the catalyst. When the CH_4/O_2 feed ratio was switched to 1.5, the combustion of part of the coke deposits on the catalyst started, temporarily giving apparent CO selectivities greater than 100%. Finally, when the original ratio of 2 was restored, the reaction rate also went back to approximately its original value, without the drop observed on the fresh catalyst (Fig. 5). Very similar results (not shown) were obtained with the Co/MgO catalyst. At a CH_4/O_2 ratio of 2 the methane conversion was approximately 92.5%; a large amount of coke was formed when the CH_4/O_2 ratio was increased to 2.5, and part of this coke was burnt when the ratio was switched to 1.5. Upon resuming the original feed ratio of 2, the conversion had dropped to values around 87%, and deposits of solid material were clearly visible in the upper section of the reactor. When the same catalyst was loaded onto a clean reactor, the original 92–93% conversion level at a CH_4/O_2 ratio of 2 was reestablished.

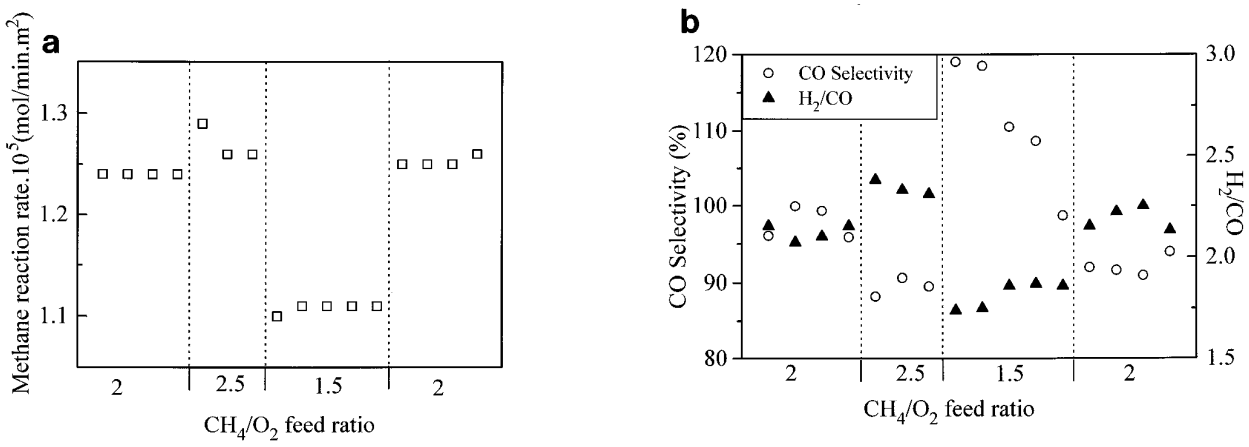

FIG. 7. Methane conversion (a) and CO selectivities and H_2/CO ratio (b), obtained with an aged Ni/MgO catalyst for different values of the CH_4/O_2 feed ratio.

DISCUSSION

The fresh catalysts containing either Ni or Co are made up of a mixture of crystalline MMgO$_2$ and MgO (M = Ni or Co), while single transition metal oxides could not be detected.The X-ray patterns (Table 2), the low reducibility of the fresh catalysts (TPR results, Table 2), the BEs of Ni2$p_{3/2}$ and Co2$p_{3/2}$ peaks and the catalytic behavior shown in Fig. 3 for fresh solids are all consistent with the above statement.

Once the catalysts reach reaction temperatures of about 800–850°C, they become partially reduced, and metallic centers are generated on their surfaces, with a sharp increase in the overall activity (Fig. 3), and in the selectivities for both CO and H_2 which reach values very close to equilibrium. These findings were confirmed by the TPR and XRD data (Table 2) and supported by the XPS data (Table 3).

The results reported by Dissanayake *et al.* (4) on Ni/Al_2O_3 are useful to explain the above findings for MgO-supported catalysts. Using a fixed-bed tubular reactor they found that, under steady-state operation, the catalyst bed had three well-defined zones. The first zone at the entrance of the reacting mixture was made up of $NiAl_2O_4$ with only moderate activity for more methane combustion to CO_2 and H_2O. The second zone, where the methane was completely burnt in a highly exothermic process, contained NiO/Al_2O_3. The exit zone, in contact with an oxygen-free atmosphere, contained essentially Ni/Al_2O_3 catalyst. In this zone CO and H_2 were formed at near equilibrium concentrations via the endothermic reforming reactions.

In the fluid-bed reactor there also exists a zone, near the distributor plate, in which the catalyst sees a highly oxidant mixture, and a second zone, which is located further into the bed, in which the oxygen has been consumed and metallic centers are produced on the solid. The main difference is, however, that the catalyst is in a permanent circulation between both zones. Thus, the Ni and Co are permanently changing between these oxidation states. These continuous redox cycles may affect the stability and catalytic behavior of these solids in the long run, a question which has not been addressed here but which may become an important subject in future research on this or analogous systems.

An estimation of the amounts of cobalt oxide and nickel oxides formed in these solids has been obtained from the TPR results in Table 2. Since these measurements were performed after burning the coke in O_2 at 500°C, the data obtained represent an average of the relative amounts of the single oxides on the whole of the catalyst bed.

A valuable advantage of the fluid bed reactor is the much lower amounts of coke measured on the used catalyst when compared to the fixed-bed operation, especially in the case of supported nickel catalysts (14). This is a consequence of the permanent circulation of the solid which is periodically transported to the oxygen-rich entrance zone of the bed, where gasification processes involving oxygen and possibly steam (from the combustion of methane), help to control the level of coke on the catalyst.

The results presented above show that cycling the catalyst between feed ratios that give rise to substantial coke buildup on the catalyst (e.g., CH_4/O_2 ratios higher than 2.5), and feed ratios that rapidly remove these coke deposits (e.g., a CH_4/O_2 ratio of 1.5), leads to a considerable drop in conversions (from 92–93% to about 80%). Also, it was shown that this reduction cannot be explained by catalyst deactivation, since inside the bubbling bed the original conversion level is still achieved, but by back reactions occurring in the freeboard, which are catalyzed by the solid deposits on the freeboard walls of the reactor,

which, for the case of Ni/MgO catalysts were analyzed and found to contain a higher proportion of nickel than the original catalyst.

On a normal fluidized bed operation it is expected that catalyst fines are generated, and part of this catalyst dust can be deposited on the freeboard walls. This, however, would give rise to small deposits, with the same composition than the original catalyst, rather than to larger, metal-enriched deposits. How these deposits are formed is hinted by the experiment reported in Fig. 5. Working at high CH_4/O_2 ratios favors the formation of coke on the surface of the catalyst. It is known that this coke forms patches and/or whiskers, which contain metal (nickel or cobalt) crystallites at the top of the filament (Fig. 2). Shifting to a more oxidating atmosphere ($CH_4/O_2 = 1.5$) favors the burning of part of the coke whiskers, with the consequent release of fine metal particles which are entrained in the gas stream. In the freeboard, the gas velocity is lower, and some of these particles can be deposited on the reactor walls. This would explain why inside the fluidized bed the conversion is still at the equilibrium value, while at the exit of the freeboard it has dropped to 80%.

Although the formation of carbonyls of Co or Ni can be responsible, at least in part, for metal losses from the catalyst, it should be noted that their formation is thermodynamically unfavorable under the high operating temperatures of the reactor. In addition, the fact that cycling between high and low CH_4/O_2 ratios does not lead to lower conversions and selectivities when an aged catalyst is employed, also suggests the participation of whiskers in the formation of coke deposits on the reactor walls, since other results in our laboratory (20) indicate that catalyst aging often leads to the loss of whisker-forming sites on the catalytic surface.

CONCLUSIONS

—The fluidized bed reactor is a very useful tool for laboratory studies in this system, due to the temperature homogeneity achieved. The low formation of coke on the catalyst surface is another key advantage of this system.

—The activation of the solid on stream has been understood in terms of the phase transformation occurring on the solid (relating to cobalt and nickel oxides). In a fluidized bed reactor different catalyst phases exist in (and are circulated between) different regions of the bed.

—Cycling the feed composition between high and low CH_4/O_2 ratios led to decreased conversions and selectivities at the reactor exit. This has been related to the formation of metal-containing deposits on the catalyst wall, very likely aided by the release of metal particles during the combustion of coke deposits as filaments (whiskers) on the catalyst.

ACKNOWLEDGMENTS

Financial support for this research was partly provided by the Ibero-American Cooperation Institute and DGICYT (Project PB93-0311). We also thank the Japan International Cooperation Agency (JICA) for the donation of the XPS Spectrometer and the X-ray diffractometer.

REFERENCES

1. J. Coronas, M. Menéndez, and J. Santamaría, *Chem. Eng. Sci.* **49,** 2015 (1994).
2. S. Irusta, E. Lombardo, and E. Miró, *Catal. Lett.,* **29,** 339 (1994).
3. A. T. Ashcroft, A. K. Cheetham, J. S. Foord, M. L. H. Green, C. P. Grey, A. J. Murrell, and P. D. F. Vernon, *Nature* **344,** 319 (1990).
4. D. Dissanayake, M. P. Rosynek, K. C. C. Kharas, and J. H. Lunsford, *J. Catal.* **132,** 117 (1991).
5. D. A. Hickman and L. D. Schmidt, *J. Catal.* **138,** 267 (1992).
6. D. A. Hickman and L. D. Schmidt, *J. Catal.* **136,** 300 (1992).
7. T. S. Christensen and I. I. Primdahl, *Hydrocarbon Process.* **73,** 3 (1994).
8. A. Santos, J. Coronas, M. Menéndez, and J. Santamaría, *Catal. Lett.* **30,** 189 (1995).
9. P. M. Torniainen, X. Chu, and L. D. Schmidt, *J. Catal.* **146,** 1 (1994).
10. W. J. M. Vermeiren, E. Blomsma, and P. A. Jacobs, *Catal. Today* **13,** 427 (1992).
11. F. van Looij, J. C. van Giezen, E. Dorrestijn, and J. W. Geus, "Proc. 4th Eur. Workshop on Methane Activation," Eindhoven, 1994.
12. M. Pettre, Ch. Eichner, and M. Perrin, *Trans. Faraday Soc.* **43,** 335 (1946).
13. Y. F. Chang and H. Heinemann, *Catal. Lett.* **21,** 215 (1993).
14. J. B. Claridge, M. L. H. Green, S. C. Tsang, A. P. E. York, A. T. Ashcroft, and P. D. Battle, *Catal. Lett.* **22,** 299 (1993).
15. U. Olsbye, E. Tangstad, and I. M. Dahl, *in* "Natural Gas Conversion II" (H. E. Curry-Hyde and R. F. Rowe, Eds.), pp. 303–308, Elsevier, Amsterdam/New York, 1994.
16. A. Santos, M. Menéndez, and J. Santamaría, *Catal. Today* **21,** 481 (1994).
17. S. S. Bharadwaj and L. D. Schmidt, *J. Catal.* **146,** 11 (1994).
18. V. R. Choudhary, A. M. Rajput and V. H. Rane, *Catal. Lett.* **16,** 269 (1992).
19. V. R. Choudhary, A. M. Rajput and B. Prabhakar, *J. Catal.* **139,** 326 (1993).
20. J. A. Peña, A. Monzón, and J. Santamaría, manuscript in preparation.
21. C. Padró, W. Grosso, G. Baronetti, A. Castro, and O. Scelza, *Stud. Surf. Sci. Catal.* **82,** 411 (1994).